Est. 1984

ORIENTAL JOURNAL OF CHEMISTRY
An International Open Access, Peer Reviewed Research Journal

www.orientjchem.org

ISSN: 0970-020 X
CODEN: OJCHEG
2022, Vol. 38, No.(1):
Pg. 44-55

Anti-metal Deteriorating and Antiviral Potency of a Novel Polynuclear Schiff base, Derived from Anthrone

SHAJU KANIMANGALATH SHANMUGHAN[1], BINDU THOZHUTHUMPARAMBIL KRISHNAKUTTY[2]*, VINOD PALAYOOR RAPHAEL[3] and JOBY THOMAS KAKKASERY[4]

[1,2,3]Department of Chemistry, Government Engineering College, Thrissur
(Affiliated to APJ Abdul Kalam Technological University) Kerala-680009, India.
[4]Department of Chemistry, St.Thomas' College (Autonomous) Thrissur, Kerala, India.
*Corresponding Author E-mail: bindujayantk@gmail.com

http://dx.doi.org/10.13005/ojc/380105

(Received: January 11, 2022; Accepted: February 17, 2022)

ABSTRACT

The versatile behavior of many Schiff bases is due to the presence of the azomethine group. In this work, we synthesized a novel polynuclear Schiff base [ANHIS] derived from anthrone and histidine, characterized using spectroscopic tools, and evaluated its anti-corrosion and anti-viral potencies. Conventional weight-loss method, electrochemical impedance spectroscopic investigation (EIS), potentiodynamic polarization studies (Tafel), adsorption studies, and quantum chemical calculations were used to investigate the anticorrosion behavior. The result showed that the Schiff base interacted with the surface metal atoms and provides good protection to the carbon steel surface against corrosion in an acid medium. A mixed-type inhibitor action of ANHIS was determined by Tafel plot analysis. A plausible mechanism of inhibition action is also anticipated. SEM analyses were carried out to explore the surface characteristics of the metal in the absence and presence of ANHIS. Drug likeness and ADMET properties of ANHIS were screened using online web servers. The preliminary IN SILICO pharmacokinetics and medicinal chemistry studies revealed that the molecule shows a very good drug-like property. The toxicity studies predict that it has less or no toxic behavior (carcinogenic in mice and non-carcinogenic in rats). The antiviral activity of the molecule was investigated on SARS-CoV-2(COVID-19 virus) using Autodock software. Docking studies showed that the polynuclear molecule ANHIS possessed hydrogen bonding, aromatic and hydrophobic interactions with the binding site of the main receptor of the COVID-19 virus. The docking score is comparable with the score value of anti-HIV drugs such as lopinavir and indinavir.

Keywords: Carbon steel, Schiff base, Corrosion inhibitors, Impedance, Drug-likeness, Docking.

INTRODUCTION

Compounds containing a carbon-nitrogen double bond (>C=N) are classified as Schiff bases (imines) and are formed by the condensation reaction of aliphatic or aromatic carbonyl compounds, with an aliphatic or aromatic primary amine. Significantly, they have wide applications in Coordination chemistry, Analytical Chemistry, Pharmaceutical chemistry, and Metal industries. This also includes

the field-biological activities like antibacterial, antifungal, anticancer, anti-inflammatory, antioxidant, and antiviral. Interestingly, previous research reports[1-13] has already shown that a Schiff base having multiple abilities should possess a lone pair of electrons and aromatic. This characteristic feature of the Schiff base enables it to act as chelating agents, corrosion inhibitors, and even antimicrobial agents. In this research work, a compound[14] was synthesized which is relatively inexpensive, eco-friendly[15,16] and yet has a special characteristic feature required for an active Schiff base. The present study aims at synthesizing a novel Schiff base molecule, characterizing and examining the applicability of this molecule concerning two factors. One is the corrosion inhibition factor (related to the metal industry) and the other is the biological factor (antiviral activity).

In carbon steel Industries, the excessive use of acidsfor pickling, de-scaling, and surface cleaning process causes to increases the dissolution rate. Related to this issue, anticorrosion agents (inhibitors) are widely applied to reduce metal deterioration rate[17-19] in the acidic medium. The corrosion inhibitors are organic molecules containing hetero atoms, aromatic rings and π-bond conjugated system. Since π-orbital can easily interact with the metal surface[20], the corrosion inhibition process effectively takes place by molecules with π-bonds. Moreover, organic molecules containing azomethine linkages were also reported as effective potential corrosion inhibitors[21-22]. The recent trend is to develop non-toxic or low toxic inhibitors at the application level. Organic molecules interact with the surface of the metal by replacing chloride ions, hydroxyl ions, and water molecules and thereby blocking the active sites for corrosion reaction.

It is an accepted fact that COVID-19 disease[23] has claimed so many precious lives. It has a great negative impact on the health andsocio-economic wellbeing of millions of people. Therefore it is of great significance to focus on the relevance of Schiff base compounds and related characteristic features in sorting out this issue. Though the researchers and medical practitioners are struggling to find a solution to handle this pandemic situation, no precise remedy to wipe away this disease and related issues till date. Even though several clinical trials are going on in different parts of the world, a well-defined treatment plan is yet to be developed. Lack of in-depth knowledge about the newly emerging virus and its interaction with human cells has placed so many limitations on finding effective treatments. Pharmaceutical companies are trying hard to explore the potency of existing antivirals/ FDA-approved drugs against the covid-19 virus. Naturally, the focus was placed on the study of the antiviral activity of a synthesized Schiff base molecule against the coronavirus. The COVID-19 infected people would experience gentle respiratory illness[24] especially upper respiratory tractand may recover after some dayswith normal treatment. Serious illness[25,26] may occur in aged people and patients suffering from other diseases like cancer, heart problems, diabetes and severe respiratory disease.Taking into consideration all these factors, it is of vital importance to develop a drug to destroy the coronavirus which otherwise will pose a life threat to numerous COVID-19 patients. In many countries, approval has been given to the existing antiviral drugs such as Favipiravir, Remdesivir, Hydroxychloroquine, Lopinavir, Indinavir, Ritonavir, etc.[27] for the treatment of COVID-19 disease.

Anticipating the use of Schiff base molecules in developing a drug meant for antiviral use it was decided to examine whether the synthesized Schiff base has the potential to act as a drug molecule or not. With focus given to this aspect, Schiff base was screened with Lipinski's rule of 5, drug-likeness[28], and ADMET[29,30] properties. In this way, the consequent safety measures were also taken into consideration. By the use of in silico concept[31-33], a study was made on the drug ability of ligand (hit-to-lead). For this, the orientation and conformation of a ligand within a protein receptor were examined by molecular docking studies. Consequently, the above study enabled the prediction of the protein–inhibitor interactions and the related structural features of the protein's active site.

With this background the synthesis of a polynuclear Schiff base containing both π-orbital & azomethine linkages was derived from anthrone and histidine and examined its inhibiting capacity against metal deterioration and virus infection. Following this, the corrosion (metal deterioration) inhibition capacity for metal (CS) in 1M HCl was examined by gravimetric measurements, impedance & polarization analysis, and quantum chemical studies. The next step focused

on the drug-likeness and ADMET profile of the Schiff base. This was carried out by computational methods using Swiss ADME. Culminating the above-mentioned factors a study was made on the antiviral activity against coronavirus using molecular docking with Auto dock softwares[34-38].

MATERIALS AND METHODS

Synthesis of imine

A hot 1:1 ethanolic solution (25 mL) of histidine (2mM) was mixed with a refluxing solution of anthrone (2mM) in ethanol (25 mL) and the refluxing continued for six hours, cooled by keeping overnight to get yellow-colored Schiff base (ANHIS) compound, filtered, washed and dried.

Characterization of Schiff base

The Schiff base was characterized by elemental analysis (Vario EL III model CHN analyzer), UV-Visible spectrum (a Shimadzu UV-Visible-1800 Spectrophotometer), and IR spectrum (Shimadzu-Model IR affinity). ^{1}H NMR (300 MHz) and ^{13}C NMR (75 MHz) spectra were recorded in DMSO-d6 on a Bruker AMX-400 NMR spectrometer.

Corrosion inhibition Studies

Inhibitor and Solutions

Poly nuclear Schiff base (ANHIS) was used as an inhibitor. The inhibitor solutions are prepared in different concentrations in HCl medium. The concentration range (0.2mM-1.0mM) of the inhibitor solutions prepared in 1M HCl medium lies in the range of.

Gravimetric studies

The metal specimen selected for the gravimetric study was carbon steel. The composition of the CS (carbon steel) were found out from SEM-EDX analysis and the values are C, 0.6%; Mn, 0.06%; P, 0.03%; S, 0.016%; Si, 0.03% and the remainder Fe. The area and thickness of the polished metal specimens (1.5 x 2 x 0.1 cm) were measured accurately, washed and dried. The weight of the dried metal coupons was found and then immersed in 50 mL acid solutions with and without ANHIS (naturally aerated) using hooks and fishing lines at 30^{0}C. The mass (weight) losses of the metal coupons were determined after 24 hours.Rate of corrosion (ν) and inhibition efficacy (η_w%) were determined by the following equations[54,55]

$$\nu = \frac{W}{St} \quad (1)$$

$$\eta_w\% = \frac{\nu_o - \nu}{\nu_o} X100 \quad (2)$$

Where 'W' is the mass of the metal lost (g), 'S' is the surface area (cm^2) of steel coupons, 't' is the period of immersion (24 h), 'ν' and 'ν_0' represent the metal dissolution rate with and without ANHIS respectively.

Impedance and polarization measurements

Impedance & polarization (electrochemical) studies were conducted in a conventional electrochemical cell with a three-electrode assembly. This three electrode system consists of a working electrode (steel specimen of exposed area-1cm^2), a counter electrode (platinum, surface area-1cm^2) and a reference (Saturated calomel).Ivium Compactstat-e workstation was employed to carry out the electrochemical investigations.

The electrochemical impedance spectroscopy (EIS) analysis was executed in the frequency range 1 kHz-100 MHz after establishing a steady-state open circuit potential. The EIS measurements provide the charge transfer resistance values and the inhibition efficiency can be found using these values. The equation relating the inhibition efficiency and charge transfer values are given below.[56]

$$\eta_{EIS}\% = \frac{R_{ct} - R'_{ct}}{R_{ct}} X100 \quad (3)$$

R_{ct} and R'_{ct} represent charge transfer resistances of the working electrodedipped in HCl in the presence and absence of ANHIS respectively. Polarization measurements were conducted in the potential range -100 to +100 mV of steel electrode with a constant sweep rate (1mV/sec). From the Tafel analysis, the value of corrosion current densities (I_{corr}) can be found out and the efficiency of inhibition ($\eta_{pol\%}$) drawn out by the use of the following relation.[57]

$$\eta_{pol}\% = \frac{I_{corr} - I'_{corr}}{I_{corr}} X100 \quad (4)$$

Where I'_{corr} and I_{corr} represent the current densities of corrosion without ANHIS & with ANHIS.

Scanning electron microscopy

During the corrosion process, the surface

texture of the carbon steel specimen was changed and the morphology was analyzed using a scanning electron microscope (model Hitachi SU6600). The surface morphology of the polished metal specimen, metal treated with acid (24 h) and corrosion inhibited metal (1mM ANHIS) were analyzed for comparison.

Quantum chemical calculations

The inhibitor ANHIS molecule was optimized by B3YLP Density Functional Theory (DFT) with GAMESS software. This quantum chemical calculation provided accurate geometry and electronic properties of the inhibitor.

Drug likeness and ADMET studies

The molecular properties and drug-likeness of ANHIS were evaluated using the online web tool (http://swissadme.ch.) The drug-like property of a candidate moleculeis expressed in terms of drug-likeness.The structure and molecular properties have an important role to predict the similarity with the existing drugs. Molecular properties like molecule size, hydrophobicity, electronic distribution, hydrogen bonding characteristics, and different pharmacophore features have control over the performance of the molecule in the living organism. The properties of the molecule ANHIS related to drug-likeness have been assessed using Swiss ADME. By drawing and submitting the Schiff base molecule's structure into the designated window, the Swiss ADME program performs the calculation. The results are loaded on the same web page. The selected compound ANHIS was subjected to toxicity predictions using the online software PreAdmet (https://preadmet.bmdrc.kr/toxicity/). The molecular structure is the key factor in determining the toxicity properties of the investigated molecule.

Molecular docking studies

Molecular docking aims to give a prediction of ligand-receptor complex structure using computational methods. The molecular docking studies help to understand the behavior of Schiff base molecule ANHIS in the binding site of corona virus main protease (Covid-19). For this purpose, the molecule ANHIS was drawn in the Chemdraw program and its geometry and energy were minimized. The optimized ligand ANHIS was saved in pdb format. Protein structure was (PDB id: 6LU7)[58] downloaded from the protein data bank and prepared before docking by removing all water molecules and adding hydrogen atoms to the receptor molecule. The protein (protease) and ligand (ANHIS) were subjected to docking studies using AUTODOCK docking software[34-36]. Using the docked output file, analysis of results was carried[37,38] out using Biovia Discovery Studio software.

RESULTS AND DISCUSSION

Structure of imine

The structure of molecule ANHIS was confirmed by CHN and spectroscopic techniques. The Fig.1 represents the structure and 3D geometry of ANHIS. The results are summarized as follows. ANHIS: CHN Analysis: Calculated (found) for $C_{20}H_{17}N_3O_2$: C, 72.42 (74.16), H, 5.13 (5.03); N, 12.67(5.03)%. Melting Point=245^{0}C; FTIR:ν_{COOH}= 1488 cm^{-1}, $\nu_{C=N}$=1612 cm^{-1}.^{1}Hnmr: δ_{COOH}=11.1, δ_{NH}=6.96 13Cnmr: δ_{COOH}=182.11, $\delta_{C=N}$=148.8ppm.

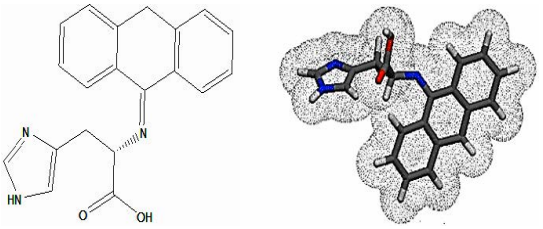

Fig. 1. Structure of ANHIS and its 3D geometry

Corrosion Inhibition Studies

Gravimetric studies

Weight loss of CS specimens in a medium of different amounts of ANHIS in 1M HCl at 30^{o}C was determined at 24 hours. Table 1 reports various corrosion parameters like corrosion rates of CS, surface coverage (θ) and inhibition efficiencies of ANHIS. Data established that, from 0 to 0.2mM inhibitor concentration, there is a sharp decrease in the corrosion rate. But a gradual lowering in the rate of corrosion was noted from 0.2mM to 1mM.

Table 1: Corrosion rates of metal, inhibition efficiencies (η_w%) of ANHIS in 1.0 M HCl and surface coverage (θ)

Con. (mM)	Rate of (mm/y) corrosion	Inhibition efficacy (η_w%)	θ
Blank	6.50	-	-
0.2	1.60	75.46	0.75
0.4	1.28	80.31	0.80
0.6	0.92	85.91	0.86
0.8	0.79	87.80	0.88
1.0	0.47	92.75	0.93

As the concentration increases, the surface converges by the inhibitor through adsorption increases and thus blocking the active sites which are vulnerable to corrosion reaction. The maximum η_W% (92.75) at 1mM clearly establishes that ANHIS acts as an effective anticorrosion agent for carbon steel in HCl medium.

Adsororptionmodeling studies

The mechanism of adsorption by ANHIS molecules can be effortlesslyunderstood by drawing the suitable adsorption isotherm. Various adsorption isotherms were drawn and the isotherm with a straight line and correlation coefficient (R^2) very close to unity is considered as the best fitted adsorption isotherm. Among the isotherms studied, Langmuir adsorption isotherm was best suited and the model is represented as[39]

Langmuir adsorption isotherm $\frac{C}{\theta} = \frac{1}{K_{ads}} + C$ (5)

Where 'C', 'θ', and 'K_{ads}' are the concentration of ANHIS, fractional surface coverage by ANHIS on CS and adsorption equilibrium constantrespectively. The Langmuir adsorption isotherm for ANHIS on the steel surface in an acid medium is depicted in Figure 2.

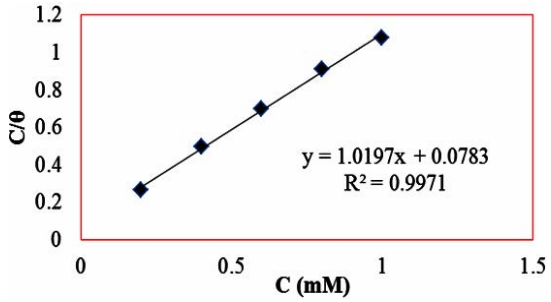

Fig. 2. Langmuir adsorption plot of ANHIS on CS

From Langmuir isotherm, the value of Kadsis found to be 490.7 and the corresponding value of standard free energy of adsorption(ΔG^0_{ads}) was -33.89 kJ/mol; which was calculated by the following equation

$\Delta G^0_{ads} = -RT\ln(55.5\ K_{ads})$ (6)

Here, R and T represent the universal gas constant and the temperature (K) respectively. The multiplication factor 55.5denotes the molar concentration of water. ΔG^0_{ads} for ANHIS on carbon steel displayed a negative value indicating that the adsorption of ANHIS on the metal surface is spontaneous.The value of ΔG^0_{ads} established that the interaction between the ANHIS molecules and the metal was electrostatic and chemical in nature.

EIS measurements

Electrochemical Impedance Spectroscopy (EIS) is a versatile tool to study the inhibition effect of ANHIS on CS surface. Nyquist plot for the CS specimen in 1M HCl containing different amounts of ANHIS is depicted in Fig. 3. The similarity of Nyquist plots revealed that the corrosion mechanism remains unaltered by the addition of inhibitor.

The impedance (both the resistive and capacitive) behavior of solution-metal interface in the presence of various concentrations of ANHIS can be well explained with Randles equivalent circuit[40]. This simple equivalent circuit fits many electrochemical systems in an acid medium. This model facilitates the calculation of electrochemical data of the corroding system under examination. The circuit (Fig. 4) consists of R_{ct} and CPE in parallel combination which is connected in series with R_s (solution resistance). Instead of double layer capacitance, a constant phase element (CPE) is employed in the circuit for minimizing the metal surface irregularities. The impedance of CPE is expressed as.

$$Z_{CPE} = \frac{1}{Y_0\ (j\omega)^n} \quad (7)$$

Where Y_0, j, n, and ω are constant of CPE, imaginary number, phase shift (exponent) and angular frequency respectively[40]. The observed impedance parameters and the inhibition ($\eta_{EIS\%}$) of ANHIS on CS surface are listed in the Table 2.

Table 2: EIS parametersof ANHIS on CS surface

Con. (mM)	R_{ct}(Ωcm²)	C_{dl}(μF cm^{-2})	ηEIS%
Blank	15.7	104	-
0.2	109.2	101.2	85.62
0.4	151.2	97.2	89.62
0.6	181.0	90.3	91.33
0.8	275.8	86.8	94.31
1.0	280.0	81.4	94.39

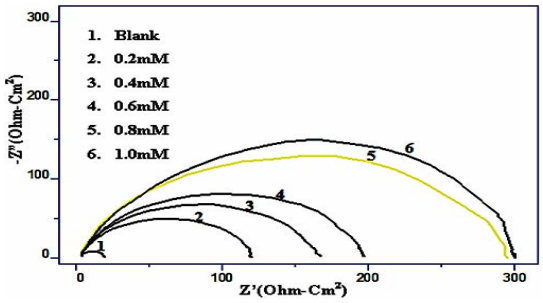

Fig. 3. Nyquist Plot of CS in HCl without and with ANHIS

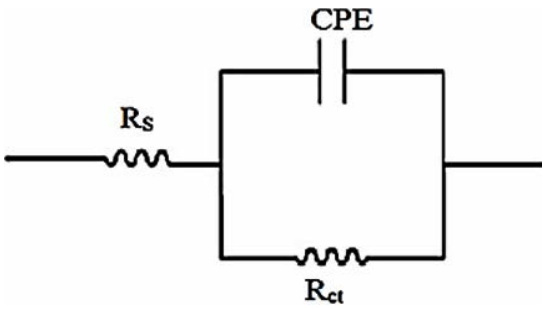

Fig. 4. Randles equivalent circuit fitting for EIS measurements

From Table 2 it is clear that the R_{ct} value increases with increase in ANHIS concentration. This finding predicts that ANHIS molecules interacted with metal by adsorption at the metal/solution interface[41] and slows down the charge transfer reaction rate which in turn decreases the corrosion rate. As the concentration of ANHIS increases, the value of C_{dl} decreases. This can be attributed to the increases in the width of the adsorbed layer. Consequently, a notable rise in the inhibition efficacy was observed with the concentration of ANHIS. These observations also support the mechanism of corrosion inhibition of ANHIS on CS that is adsorption. A maximum of 94.39% inhibition efficiency was achieved for ANHIS on the carbon steel specimen at a concentration of 1mM.

Tafel polarization investigations

Figure 5 represents Tafel curves for CS in HCl at 30^{0}C in the presence and absence of ANHIS (0 to 1mM concentration). Table 3 furnishes the basic Tafel parameters like corrosion potential (E_{corr}), corrosion current density (I_{corr}), cathodic (b_c) and anodic (b_a) Tafel slopes, and inhibition efficiency ($\eta_{pol\%}$) of ANHIS on carbon steel specimens. The data show that the adding of ANHIS to the HCl medium affects both the anodic and cathodic regions of the slopes. Table 3 clearly indicates the marked difference in corrosion current densities of inhibited and uninhibited solutions. This is due to the interaction of ANHIS molecules on the CS surface through adsorption. The decrease in the I_{corr} value is more at high ANHIS concentration and high inhibition efficiency was obtained (93.12%) for 1mM inhibitor concentration. Furthermore, the addition of ANHIS did not change the value of E_{corr} significantly (shift of E_{corr} is less than 85)[42] which suggests that ANHIS inhibits both anodic and cathodic processes of corrosion (mixed type).

Table 3: Tafel parameters of CS in the absence and presence of ANHIS

	Tafel Data				
C (mM)	E_{corr} (mV/SCE)	I_{corr} (mA/cm^2)	b_a (V/dec)	$-b_c$ (V/dec)	$\eta_{pol\%}$
Blank	-489	0.6282	0.076	0.096	-
0.2	-486	0.1160	0.078	0.082	81.53
0.4	-490	0.0817	0.076	0.084	86.99
0.6	-488	0.0706	0.074	0.081	88.76
0.8	-489	0.0479	0.073	0.085	92.38
1.0	-492	0.0432	0.076	0.079	93.12

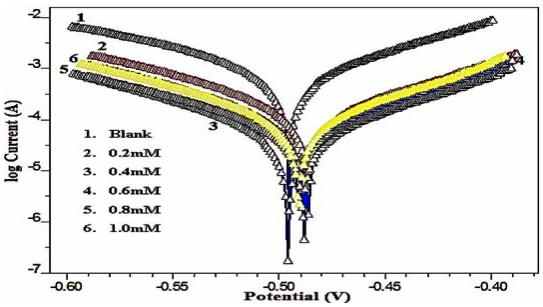

Fig. 5. Tafel plot of CS in the absence and presence of ANHIS

Surface morphological studies

The SEM images of the smoothened CS surface, corroded surface in HCl and ANHIS (1mM) adsorbed surface are depicted in Fig. 6. From Fig. 6B it is clear that the CS surface has undergone severe corrosion in the absence of ANHIS. But the surface of CS is greatly protected by the addition of ANHIS as shown by image 6C. These findings support that the molecule ANHIS molecules adsorbed on CS surface act as a protective barrier against corrosion in HCl medium.

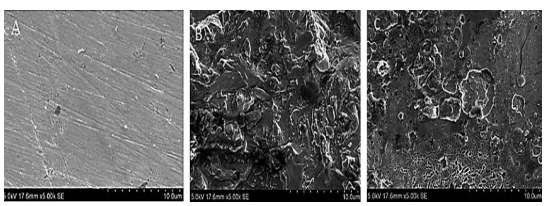

Fig. 6. SEM images of CS surfaces: A) Smoothened surface, B) Corroded surface in HCl C) ANHIS (1mM) adsorbed surface

Mechanism of Inhibition

The adsorption and electrochemical studies revealed the potency of ANHIS to mitigate the acid corrosion by adsorption on the metal surface. The mechanism of adsorption of ANHIS on CS surface may be viewed by the following model. The Schiff base ANHIS in the acid medium easily undergoes protonation and the molecule exists in the cationic form $[ANHIS\text{-}H]^+$. In general, the surface of the metal is negatively charged due to the adsorbed chloride ion originated from HCl. The electrostatic force of attraction between protonated Schiff base $[ANHIS\text{-}H]^+$ and the metal surface caused the strong adsorption of imines[42].

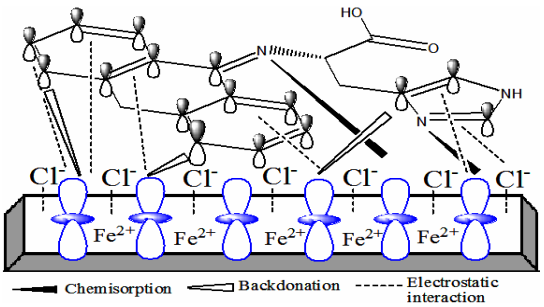

Fig. 7. Schematic representation of possible interactions between ANHIS and Fe metal surface

Besides this interaction (physisorption), chemical interaction (chemisorption) is also possible via transferring of an unshared electron pair of the Schiff base to the empty d-orbital of metal atoms. Other possible interactions during the adsorption process are the interaction between π-electrons (from aromatic & azomethine linkage) of ANHIS with d-orbital of the Fe atoms and the back donation of the d-orbital electron to empty antibonding molecular orbitals of ANHIS. The Schematic representation of different interactions possible between ANHIS and Fe metal surface are presented in Fig. 7. In short, ANHIS molecules reduce the dissolution of Fe atom to Fe^{2+} by hindering the active sites of corrosion through adsorption.

Quantum Chemical Investigations

The inhibition efficacy of ANHIS was correlated with the structural parameters using quantum chemical calculations. EHOMO, ELUMO and their difference (ΔE) are the very important quantum chemical parameters. These parameters of ANHIS are given in Table 4. The highest and lowest unoccupied molecular orbitals of ANHIS are shown in Fig. 8. The interaction of ANHIS on CS surface can be explained using Pearson's donor-acceptor concept (HSAB concept). The electron rich orbitals of the ANHIS, donates electrons to the d orbitals of Iron atom on the surface. This donor-acceptor interaction significantly reduces the metal dissolution. Table 4 shows electronegativity (χ) and chemical hardness (η) of ANHIS derived from HSAB theory. Determination of these parameters is possible with the help of the following equations.[43]

$$\chi \approx -1/2\ (E_{HOMO} + E_{LUMO}) \quad (8)$$

$$\eta \approx 1/2\ (E_{HOMO} - E_{LUMO}) \quad (9)$$

HOMO and LUMO has a significant role in predicting the chemical reactivity according to the frontier molecular orbital theory. Higher the value of EHOMO will favor the higher inhibition efficiency of the molecule since it is a good condition to promote electrons to the unoccupied orbital. On the other hand acceptance of electrons is greatlyachieved for ELUMO state. The smaller value of E_{LUMO}-E_{HOMO} (ΔE) enables the robust attachment of ANHIS on the steel surface. Quantum chemical parameters help to calculate the number of electrons (ΔN) transferred from the ANHIS to the CS surface. For a bulk Iron metal, chemical hardness and the electronegativity are taken as zero and 7eV respectively for the easiness of calculation[39].

Table 4: Quantum chemical parameters calculated by computational studies

E_{HOMO} (eV)	E_{LUMO} (eV)	ΔE (eV)	X	H	ΔN
-3.3715	1.2136	4.5851	1.0789	2.2925	1.2913

$$\Delta N = \frac{\chi_{Fe} - \chi_{inhib}}{2(\eta_{Fe} + \eta_{inhib})} \quad (10)$$

Equation 10 is used to determine the approximate values of electron transferred from ANHIS to metal atom. A metal immersed in an inhibitor solution can be viewed as a system containing Lewis acid (metal) and Lewis base (inhibitor). In metallic corrosion (acidic medium), the inhibitor (soft base) is more efficient since bulk metals are soft acids. Soft molecules generally have a small value of chemical hardness, low energy gap of HOMO-LUMO, and enhanced polarizability[39]. Usually they may have high chemical reactivity. Quantum chemical parameters (Table 8) derived by HSAB concept very well the inhibitory action of the molecule ANHIS. The experimental data also supports the quantum chemical calculations.

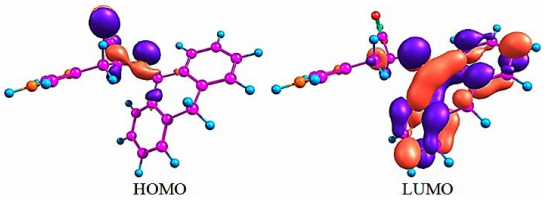

Fig. 8. HOMO and LUMO of ANHIS

Drug likeness and ADMET studies

Physicochemical properties

Table 5 displays the physicochemical parameters of the molecule ANHIS. The molecule has four hydrogen bond acceptors and two hydrogen bond donors with a molecular mass of 331.37. ANHIS satisfied the criterion for the oral bioavailability since it consists of 4 rotational bonds. The transportation of a molecule through the cellular membranes can be predicted by the Topological Polar Surface area (TPSA). This synthesized Schiff base displayed 78.34 Å²TAPSA and can be considered to have good transportation ability[44]. In general, pharmaceutically efficient molecules will not possess too or less solubility in water. Moderately soluble compounds will favor the absorption in the GI tract. *In silico* investigation showed that ANHIS possesses moderate solubility and displayed LogS of -4.28 suggesting that it is a suitable state to active in orally as well as in GI tract.

Pharmacokinetics Properties

Drug molecules which act on the Central Nervous System (CNS) will have the potency to cross the Blood-Brain Barrier (BBB). Psychiatric drugs and the number of drugs used for neuropathic diseases will act on CNS and cross BBB to combine with the target proteins present in CNS. To avoid adverse effects drugs used for diseases other than CNS related, will not cross the BBB45. It is observed from Table 5 that Schiff bases possess the power to penetrate BBB and may cause CNS side effects. The ability of ANHIS to act as agonist or antagonist for cerebral receptors has to be studied in detail. P-glycoproteins (P-gp) are acting as the defending tool for CNS from the toxins and xenobiotics[45]. ADME result shows that Schiff base is substrates of P-gp which is indicated in the Table 5.

A class of enzymes called cytochromes p450 (CYP)[46] plays an important role in the elimination of drug or toxins. A great amount of information regarding the drug-drug interactions can be drawn out by closely examining the inhibitive nature of the drug on the above isoenzymes. Due to the multi-drug interactions, accumulation of the toxins or drug metabolites originates which may create side effects. From Table 5 the results of CYP inhibitors show that Schiff base compound is found to be non-inhibitor towards isoforms of CYP. Skin Permanent ($logK_p$) value was found to be -5.91 cm/s. If the value of log K_p is more negative, skin permeability of the molecule will be less.

Table 5: The physicochemical properties of the drug candidate ANHIS

Physicochemical Properties		Pharmacokinetics	
Molecular Weight	331.37 g/mol	Skin Permanent	-5.91 cm/s
Hydrogen bond Acceptors	4 No.	P-gp Substrate	Yes
Rotatable bonds	4 No.	BBB Permeability	Yes
TPSA	78.34Å²	CYP2-CYP2D6 inhibitor	NO
Hydrogen bond donors	2 No.	CYP1-CYP2C9 inhibitor	NO
Water solubility (ESOL Class)	Moderately soluble	G I Absorption	High

Lipophilicity

Table 6 provides the Lipophilicity, Medicinal Chemistry and Drug likeness and Medicinal Chemistry properties. The coefficient LogP[47] governs the hydrophobic and hydrophilic nature of the Schiff base molecule. LogP value is a useful parameter which predicts the solubility characteristic of synthesized molecules which in turn indicates the extent of permeability through the cellular systems of living organisms. Results showed that the Log P value of Schiff base ANHIS fall within the range –0.7 to +5.0 suggesting that this molecule has appreciable permeability and oral absorption.

Drug-likeness

The drug-likeness and pharmacokinetics of a lead compound can be visualized using a set of rules made by scientists such as Lipinski, Ghose, Veber, Egan and Mugge[48]. It was found that >60% of the drugs available in the market obey these rules with slight violations. Molecular mass, LogP, number of HBD and HBA, TPSA, number of N and O are the parameters taken into account by the scientists to create the rules.

Table 6 shows that the Schiff base ANHIS obeyed all rules of drug-likeness without any

violations. This points the possibility of ANHIS and similarly structured compounds to act as the drug candidate for various diseases. The oral activity of the molecules can be further interpreted with the help of the parameter known as Abbot Bioavailability score[49]. Lipinski rule of five and TPSA of the molecule are the two important tools by which bioavailability score is calculated quantitatively. ANHIS possessed a bioavailability score of 0.55, indicating that it has the potential to act as an oral drug candidate.

Table 6: Lipophilicity, Drug likeness and Medicinal Chemistry properties of ANHIS

Lipophilicity	Druglikeness		Medicinal chemistry	
Log $P_{o/w}$ (iLOGP)	0.9 Lipinski	0	PAINS	0
WLOGP (Log $P_{o/w}$)	2.9 Veber	0	Lead-likeness	Yes
XLOGP3 (Log $P_{o/w}$)	3.4 Egan	0	Brenk	1
MLOGP (Log $P_{o/w}$)	1.8 Ghose	0	Synthetic accessibility	3.65
SILICOS-IT (Log $P_{o/w}$)	4.4 Muegge	0		
Consensus Log $P_{o/w}$	2.7 Bioavailability Score	0.55		

Medicinal Chemistry

Certain structural moieties present in the molecules may be responsible for a wrong signal on interaction with some receptors. This is termed as PAINS (Pan Assay Interference compounds)$_{50}$. In medicinal chemistry, the structural behaviour of a molecule that causes toxic or chemically unstable behaviour towards a particular receptor is evaluated by Brenk alert[51]. Table 6 shows zero PAINS alert and 1 Brenk alert for ANHIS. The synthetic accessibility score for the Schiff base molecule was found to be 3.65 and therefore possess good feasibility to synthesize. The Lead–likeness factor shown in Table 6 establishes that the molecule is susceptible to lead optimization.

Bioavailability Radar

Bioavailability radar (Fig. 9) enables us to get a piece of first-hand information regarding the drug-likeness of the molecule[52]. The suitable physicochemical space for oral bioavailability is represented by the pink-colored zone. For a molecule which shows good oral bioavailability, the molecular plot must fall correctly in the pink zone of the radar plot. The optimal range of various parameters like XLOGP3, Size, TPSA, LogS, saturation factor and flexibility are shown in the parentheses. (–0.7 and +5.0; 150 and 500 g/mol; 20 and 130Å^2; not higher than 6; not less than 0.25; not more than 9 rotatable bonds). Here XLOGP3, TPSA and LogS correspond to lipophilicity, molecular weight and solubility respectively. From the Swiss ADME prediction output (Table 5 & 6), molecule ANHIS falls in the optimal range of parameters and can be considered to have its own chemotherapeutic efficiency.

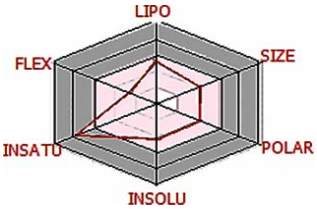

Fig. 9. Bioavailability radar

Toxicity Prediction using PreADMET

Toxicity study is a very important feature in the drug ability prediction process. It can predict whether the molecule under study is toxic or not based on carcinogenicity and mutagenicity. The mutagenicity of a compound can be generally predicted with the help of a simple test called Ames test[51]. The toxicity responsible for activating cancer in the body is termed as carcinogenicity. This toxicity test is usually carried out by exposing mice or rats to the molecule/drug candidate. The PreADMET server predicts the toxicity results from its model. Data acquired from National Toxicology Program (NTP) and USA Food and Drug Administration (FDA) is utilized for creating the toxicity models. NTP and FDA obtained these data from the results of in vivo testing of mice and rats for carcinogenicity for at least about 2 years. The Ames test prediction for the molecule ANHIS revealed that the compound is mutagenic. In the prediction of carcinogenicity in mice, the compound showed negative prediction, i.e. there is evidence of carcinogenic activities in the mouse. In the prediction of carcinogenicity in rats, the compound has shown positive prediction, i.e. it is not carcinogenic.

Molecular docking studies

The potency of small molecules to bind with the receptor proteins can be predicted with the help of molecular docking. Most suitable conformation of the molecule in the binding pocket (pose) and the binding energy of ligand-receptor complex can be evaluated with the help of docking. Docking study also enables one to identify the

various interactions possible between the ligand and receptor protein. The stability of the protein-ligand complex can be best explained using binding scores. Among the possible interactions, conventional hydrogen bonds established between the protein and the molecule greatly contribute to the binding energy. Greater the value of the binding energy (magnitude), greater will be the stability of the receptor-ligand complex. Apart from the conventional hydrogen bonding interactions[53], hydrophobic interactions like alkyl interactions and π-stacking interactions also improves the binding stability. From the computational docking studies, it is clear that the molecule ANHIS shows binding energy of -8.1kcal/mol with the main protease of coronavirus and this is comparable with the docking score of anti- HIV drugs (lopinavir and indinavir[27]) on the same receptor.

Ligand ANHIS established four conventional H-bonds with GLU166, HIS163, CYS145, and GLY143. Three hydrogen bonds were originated from the amino acid residues Gly143, Cys145 and Glu166 to the two imidazole nitrogens and C=O of the acidic group of the ANHIS respectively. ANHIS displayed one one unfavorable interaction with His41. Leu27 and His164 amino acid residues of the receptor interacted weakly with ANHIS using van der Waals forces. Fig. 10 represents the 2D and 3D interaction plots of ANHIS with the receptor. Aromatic, hydrophobic and hydrogen bond interaction profiles of Covid-19 main protease with the ligand ANHIS are shown in Figure11.

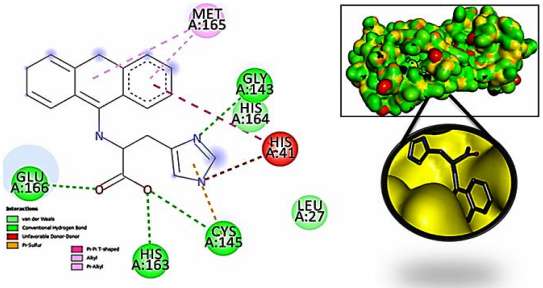

Fig. 10. 2D and 3D interaction plots of ANHIS with Covid-19 main protease

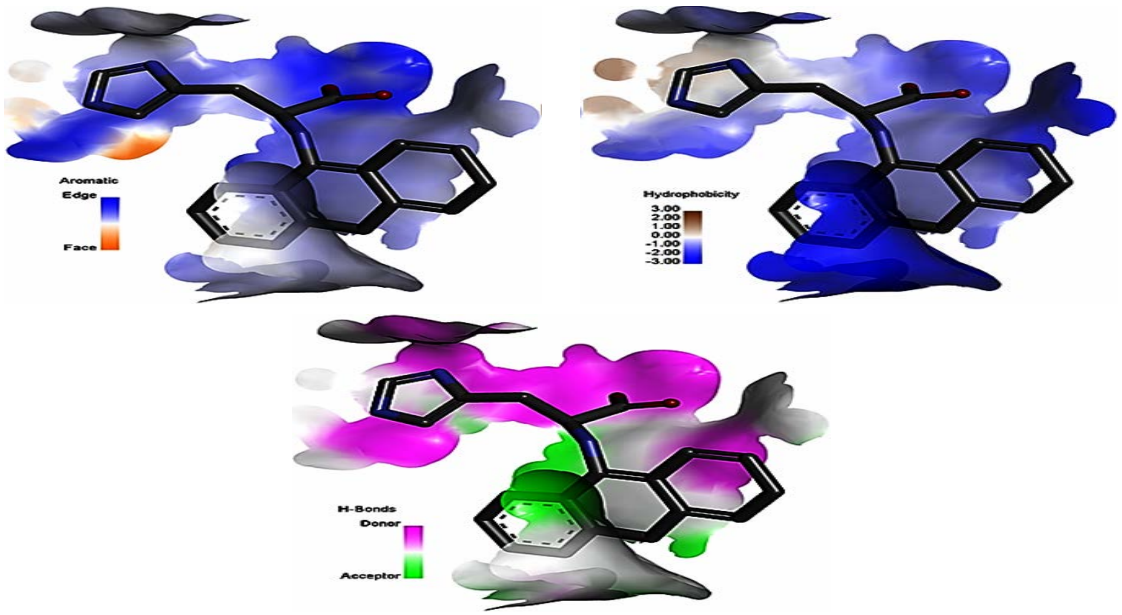

Fig. 11. Aromatic, hydrophobic and hydrogen bond interaction profiles of SARS-CoV-2 protease with ANHIS

CONCLUSION

1. The synthesized imine ANHIS prevents the dissolution of carbon steel in HCl and acts as a good corrosion inhibitor.
2. The mechanism behind the corrosion inhibition is adsorption and the molecule obeys Langmuir isotherm on the CS surface.
3. The role of ANHIS molecule at the metal/ solution interface was established by EIS studies.
4. Potency of ANHIS to interact with the anodic and cathodic process of corrosion was determined by Polarization studies.
5. SEM analysis supports the creation of a preventive layer of ANHIS on CS surface layer

which facilitates the lowering of corrosion rate.

6. The binding affinity of the molecule on the CS surface is further confirmed with quantum chemical calculations.
7. Swiss ADME prediction reveals that molecule ANHIS shows moderate water solubility, is expected to have good oral adsorption, no violation of the Lipinski rule, and drug-like properties.
8. Toxicity prediction shows that the molecule ANHIS is carcinogenic in mice and non-carcinogenic in rats.
9. In silico docking studies of ANHIS with the main protease coronavirus reveal the potency of the molecule to interact with the binding pocket of the receptor.
10. The physicochemical and medicinal chemistry properties of the molecule revealed the drug likeness of ANHIS.

ACKNOWLEDGMENT

The authors are grateful to Dr. Suseela V D for providing language help during the writing process.

Conflict of interest

The authors declare that we have no conflict of interest.

REFERENCES

1. Zhang, N.; Fan, Y.; Zhang, Z.; Zuo, J.; Zhang, P.; Wang, Q.; Liu, S.; Bi, C. *Inorg. Chem. Commun.*, **2012**, *22*, 68–72.
2. Shaju, K. S.; Thomas, K. J.; Raphael, V. P.; Paul, A. I.S.R.N. *Corros.*, **2012**, 1–8.
3. Tümer, M.; Akgün, E.; Toroğlu, S.; Kayraldiz, A.; Dönbak, L. *J. Coord. Chem.*, **2008**, *61*(18), 2935–2949.
4. Arif, M.; Qurashi, M. M. R.; Shad, M. A. *J. Coord. Chem.*, **2011**, *64*(11), 1914–1930.
5. Abdel-Rahman, L. H.; El-Khatib, R. M.; Nassr, L. A.; Abu-Dief, A. M.; Ismael, M.; Seleem, A. A. *Spectrochim. ActaA Mol. Biomol. Spectrosc.*, **2014**, *117*, 366–378.
6. Abu-Dief, A. M.; Mohamed, I. M. A. *BeniSuef Univ. J. Basic Appl. Sci.*, **2015**, *4*(2), 119–133.
7. Gehad G. M.; Omar M. M.; Ahmed M. M. *Spectrochim. ActaA Mol. Biomol. Spectrosc.*, **2005**, *62*, 1140–1150.
8. Shaju, K. S.; Joby Thomas, K.; Raphael, V. P.; Paul, A. I.S.R.N. *Electrochem.*, **2013**, 1–8.
9. Bharamagouclar T. D.; Pujar M. A.; Alagawadi A. R. *Curr. Sci.,* **1987**, *56*, 889–890.
10. Krishnan, S. K.;, Swastika, G.; Ravichandran, V.; Erik, D. C. *Eur. J. Med. Chem.*, **2010**, *45*(11), 5474–5479.
11. Chohan, Z. H. H.; Supuran, C. T. *J. Enzyme Inhib. Med. Chem.*, **2008**, *23*(2), 240–251.
12. Thomas, J.; Parameswaran, G. *Asian J. Chem.*, **2002**, *14*(3–4), 1370–1382.
13. Nair, M. S.; Arish, D.; Joseyphus, R. S. *J. Saudi Chem. Soc.*, **2012**, *16*(1), 83–88.
14. Shaju, K S.; Thomas K, J.; Raphael, V. P. *Orient. J. Chem.*, **2014**, *30*(2), 807–813.
15. Haque, J.; Srivastava, V.; Verma, C.; Quraishi, M. A. *J. Mol. Liq.*, **2017**, *225*, 848–855.
16. Abeng, F. E.; Ikpi, M. E.; Ushie, O. A.; Anadebe, V. C.; Nyong, B. E.; Obeten, M. E.; Okafor, N. A.; Chukwuike, V. I.; Nkom, P. Y. *Chem. Data Coll.*, **2021**, *34*.
17. James, A. O., Oforka N.C.; Olusegun K.A. *Int. J. Electrochem. Sci.*, **2007**, *2*, 278-284.
18. Abd El-Maksoud, S. A. *Int. J. Electrochem. Sci.*, **2008**, *3*, 528-555.
19. Suraj B. A.; Deshpande M. N.; Kolhatkar D. G. *J. Chem. Pharm. Res.*, **2012**, *4*, 1033-1035.
20. Ebenso E. E., Okafor P. C., Offiong O. E., Ita B. I., IBOK U. J.,Ekpe U. *J. Bull. Elect. Chem.,* **2001**, *17*, 459-464.
21. Sethi, T. A.; Chaturvedi, A.; Upadhyay, R. K.; Mathur, S. P. *J. Chil. Chem. Soc.,* **2007**, *52*(3), 1206-1213.
22. Srivastava K. P.; Ashwini K.; Rakesh S. *J. Chem. Pharm. Res.*, **2010**, *2*, 68-77.
23. World Health Organization (WHO). https://www.who.int/emergencies/diseases/novel-coronavirus-2019/technicalguidance/naming; World Health Organization, p **2020** the coronavirus disease (covid-2019) and the virus that causes it.
24. World Health Organization. Newsroom, Q and A on Coronaviruses (COVID-19). https://www.who.int/newsroom/q-a-detail/q-a-coronaviruses; WHO., **2020**.
25. Hui, D. S. S.; I Azhar, E.; Madani, T. A.; Ntoumi, F.; Kock, R.; Dar, O.; Ippolito, G.; Mchugh, T. D.; Memish, Z. A.; Drosten, C.; Zumla, A.; Petersen, E. *Int. J. Infect. Dis.,* **2020**, 91, 264–266.
26. Indian Council of Medical Research, Press release. Available from :(www. icmr.gov.in/media.html).

27. Raphael, V. P.; Shaju, K. S. *Indian J. Pharm. Educ. Res.*, **2020**, *54*(4), 1031-1038.
28. Lipinski, C. A. *J. Pharmacol. Toxicol. Methods.*, **2000**, *44*(1), 235–249.
29. Guan, L.; Yang, H.; Cai, Y.; Sun, L.; Di, P.; Li, W.; Liu, G.; Tang, Y. *Med. Chem. Comm.*, **2019**, *10*(1), 148–157.
30. Yang, H.; Lou, C.; Sun, L.; Li, J.; Cai, Y.; Wang, Z.; Li, W.; Liu, G.; Tang, Y. *Bioinformatics.*, **2019**, *35*(6), 1067–1069.
31. Ferreira, L. G. G.; Dos Santos, R. N.; Oliva, G.; Andricopulo, A. D. *Molecules.*, **2015**, *20*(7), 13384–13421.
32. Sliwoski, G.; Kothiwale, S.; Meiler, J.; Lowe, E. W. *Pharmacol. Rev.*, **2014**, *66*(1), 334–395.
33. The PyMOL Molecular Graphics System, version 1.2r3pre; Schrödinger, LLC.
34. Hodos, R. A., Brian A. K.;Khader S.; Ben P. R.;Joel T. D. *WIREs Syst. Biol. Med.,* **2016**, 186.
35. Biovia, D.S. *Discovery Studio Software Version V1.6.1.0.15355*; DassaultSystemes.
36. Trott, O.; Olson, A. J. *J. Comp. Chem.*, **2010**, *31*(2), 455–461.
37. Freitas D.; Ferreira R.; Schapira M. *Med. Chem. Comm.*, **2017**, *8*(10), 1970–1981.
38. Brylinski, M. *Chem. Biol. Drug Des.*, **2018**, *91*(2), 380–390.
39. Raphael, V. P.; Shanmughan, S. K.; Kakkassery, J. T. *Int. J. Corros.*, **2016**, 1–10.
40. Macdonald, J. R. *Ann. Biomed. Eng.*, **1992**, *20*, 289-305.
41. Ferreira, E. S.; Giacomelli, C.; Giacomelli, F. C.; Spinelli, A. *Mater. Chem. Phys.*, **2004**, *83*(1), 129–134.
42. Shanmughan, S. K.; Kakkassery, J. T.; Raphael, V. P.; Kuriakose, N. *Curr. Chem. Lett.*, **2015**, *4*(2), 67–76.
43. Pearson, R. G. *Inorg. Chem.*, **1988**, *27*(4), 734–740.
44. Alswaidan, I. A.; Sooknah, K.; Rhyman, L.; Parlak, C.; Ndinteh, D. T.; Elzagheid, M. I.; Ramasami, P. *Comp. Biol. Chem.*, **2017**, *68*, 56–63.
45. Ma, X. L.; Chen, C.; Yang, *J. Acta Pharmacol. Sin.*, **2005**, *26*(4), 500–512.
46. Szakács, G.; Váradi, A.; Ozvegy-Laczka, C.; Sarkadi, B. *Drug Discov. Today.*, **2008**, *13*(9–10), 379-393.
47. Ogu, C. C.; Maxa, J. L. *Proc. Bayl. Univ. Med. Cent.*, **2000**, *13*(4), 421–423.
48. Daina, A.; Michielin, O.; Zoete, V. *Sci. Rep.*, **2017**, *7*, 42717 (1-13).
49. Martin, Y. C. A. A. *J. Med. Chem.*, **2005**, *48*(9), 3164–3170.
50. Baell, J. B.; Holloway, G. A. *J. Med. Chem.,* **2010**, *53*(7), 2719–2740.
51. Ames, B. N.; Gurney, E. G.; Miller, J. A.; Bartsch, H. *Proc. Natl. Acad. Sci. U. S. A.,* **1972**, *69*(11), 3128–3132.
52. Ritchie, T. J. J.; Ertl, P.; Lewis, R. *Drug Discov. Today.*, **2011**, *16*(1–2), 65–72.
53. Raphael, V. P.; Shanmughan, S. K. *Adv. Pharmacol. Pharm. Sci.*, **2020**, 1-10,
54. ASTM G-31-72.*Standard Recommended Practice for the Laboratory Immersion Corrosion Testing of Metals; ASTM.*, **1990**, 401.
55. Emregül, K. C.; Atakol, O. *Mater. Chem. Phys.,* **2004**, *83*(2–3), 373–379.
56. Raman, A.; Labine, P. Reviews on Corrosion Inhibitor Science and Technology. *NACE1.*, **1986**, *11*, 20.
57. Ashassi-Sorkhabi, H.; Shaabani, B.; Seifzadeh, D. *Electrochim. Acta.*, **2005**, *50*(16–17), 3446–3452.
58. Protein Data Bank. PDB. ID: 6lu7. http://www.rcsb.org. https://www.rcsb.org/structure/6lu7, **2020**.